Progress In Electromagnetics Research C, Vol. 59, 21–30, 2015

Substrate Integrated Evanescent Filters Employing Coaxial Stubs

Vitaliy Zhurbenko*

Abstract—Evanescent mode substrate integrated waveguide (SIW) is one of the promising technologies for design of light-weight low-cost microwave components. Traditional realization methods used in the standard evanescent waveguide technology are often not directly applicable to SIW due to dielectric filling and small height of the waveguide. In this work, one of the realization methods of evanescent mode waveguides using a single layer substrate is considered. The method is based on the use of coaxial stubs as capacitive susceptances externally connected to a SIW. A microwave filter based on these principles is designed, fabricated, and tested. The filter exhibits a transmission zero due to the implemented stubs. The problem of evanescent mode filter analysis is formulated in terms of conventional network concepts. This formulation is then used for modelling of the filters. Strategies to further miniaturization of the microwave filter are discussed. The approach is useful in applications where a sharp roll-off at the upper stop-band is required.

1. INTRODUCTION

Evanescent mode waveguide technology allows for more compact component design in comparison to the traditional dominant mode waveguide technology [1, 2]. Evanescent microwave components can be integrated into a substrate in order to further reduce the mass and volume. Several successful attempts have been made in this direction. They are based on introducing various ridge waveguides into a multilayer substrate [3, 4] and etching split ring resonators in the metal layer of a single layer substrate integrated waveguide (SIW) [5–7]. This work investigates an alternative realization method, which is based on introducing capacitive susceptance into a SIW in a form of either lumped capacitors or coaxial stubs, as it is shown in Fig. 1. The technology relies on a single layer PCB realization and allows for relatively simple analysis. Using well described lumped capacitors or coaxial stubs as susceptances allows to avoid rigorous full-wave simulations. Implementation of coaxial stubs provides more preferable response, since they introduce transmission zeros, as it will be shown later. On the other hand, lumped capacitors allow for more compact volume of the filter, though the filter footprint remains the same. The filters are excited using a direct coaxial-to-evanescent mode SIW transition rather than the conventionally used series connection of two transitions: a coaxial-to-planar transmission line followed by a planar-to-SIW transition. According to author's knowledge, the method to integrate an evanescent mode waveguide into a single layer PCB avoiding the use of planar resonators is described here for the first time.

Having an analytical model would be beneficial for analysis of such structures. A lumped element equivalent circuit representation is traditionally used for design of evanescent filters. A correction factor Δ was used in the original paper by Craven describing the design theory [8]. This factor compensates satisfactory in moderate- to narrow-band designs [9]. A more refined method of correction involving the use of frequency transformation has been proposed later in [9]. An approach based on impedance matrix representation is used in this work for the design of evanescent waveguide filters, and is described

Received 24 June 2015, Accepted 9 August 2015, Scheduled 13 August 2015
* Corresponding author: Vitaliy Zhurbenko (vz@elektro.dtu.dk).
The author is with the Technical University of Denmark, Oersteds Plads 348, 2800 Kgs. Lyngby, Denmark.

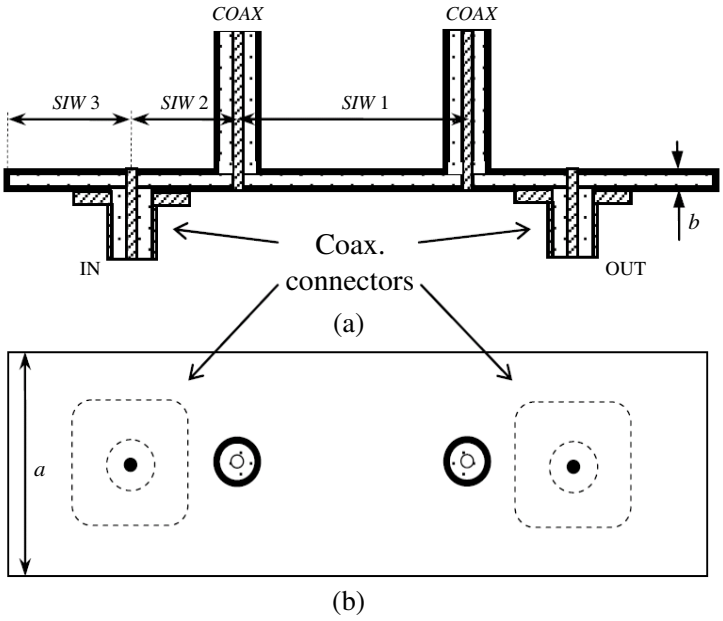

Figure 1. Evanescent mode substrate integrated waveguide filter with coaxial stubs. (a) Sketch of the filter cross-section, (b) Top view. On this sketch, a — is the wide side of the waveguide, b — is the narrow side.

in Section 3 of this paper. The developed models allow to predict the filter response in a wide frequency range. In order to validate the developed filter models as well as the realization method, a microwave filter, as the one shown in Fig. 1, is designed, fabricated and tested. The measured results are presented in Section 4. Implementation of inductive posts for stop-band improvement is discussed in Section 5.

2. EVANESCENT MODE WAVEGUIDE INTEGRATED INTO A SUBSTRATE

2.1. Integration into SIW and Susceptance Realization

A section of an evanescent mode waveguide is traditionally represented by a π-network consisting of two parallel inductors and one series [8]. The values of the inductors depend on the cross-sectional dimensions of the waveguide and the length of the section. Introducing capacitors in parallel to the parallel inductors will form two parallel LC resonators with inductive coupling between them. This will then form a conventional coupled resonator filter.

The traditional way to realize capacitive susceptance is to place capacitive posts, capacitive strips, or capacitive resonators into a waveguide [10, 11]. These solutions have proven their viability in standard waveguide technology, however, it is technologically challenging to implement in SIW. For example, capacitive posts in SIW would require a two layer PCB process. The capacitance will depend on the gap between the post and the wall of the waveguide making filter sensitive to the process variations.

One of the solutions to this is to use lumped surface mounted device (SMD) capacitors as capacitive susceptance in a SIW. The capacitors can be mounted on a surface of the PCB bringing the lower metal layer to the top layer with a metalized via hole. This, however, might introduce radiation loss due to the opening in the waveguide wall. If this opening is kept narrow and arranged along the waveguide such that it does not cross the surface current lines, the radiation loss can be minimized. Further on, the radiation loss can be completely avoided if the capacitor is inserted directly into a hole in the wide wall of a SIW, as it is shown in Fig. 2(a).

The capacitive susceptance stores the energy in the electric field, and the Q-factor of the overall structure is sensitive to the loss in the susceptance. The Q-factor provided by SMD components is insufficient in many cases resulting in high insertion loss of evanescent mode waveguide filters. Distributed components can be used to mitigate this drawback and reduce insertion loss. One of

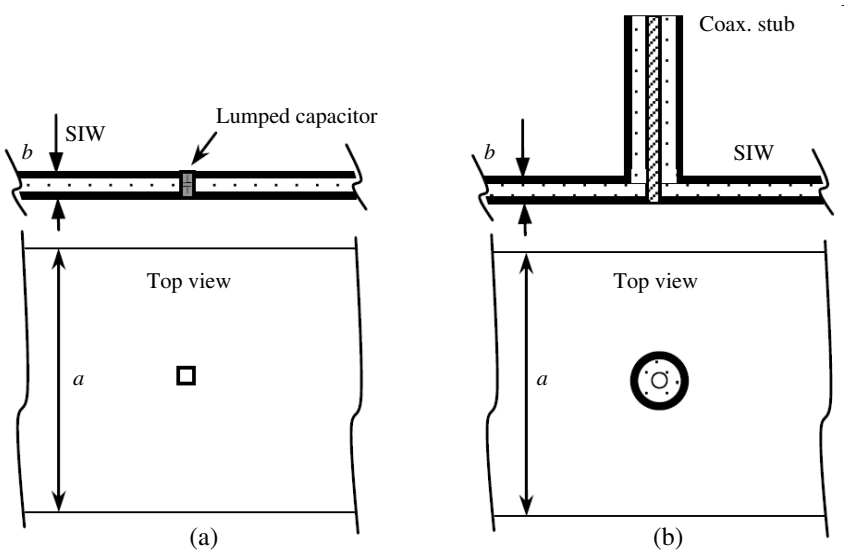

Figure 2. Capacitive susceptance in the evanescent mode SIW. Cross-section and top view. (a) Lumped capacitor; (b) Coaxial stub.

the ways to realize capacitive susceptance is to use a stub based on, for example, a section of coaxial transmission line. The centre conductor of the coaxial line should be connected to one of the wide walls of the waveguide and the outer conductor should be connected to the opposite wall, as it is shown in Fig. 2(b). Standard off-the-shelf coaxial transmission lines can be used for susceptance realization. The advantage over lumped capacitors is that the open-circuit stub can be used to realize capacitive susceptances ranging from zero to virtual infinity. In addition, the value of the stub susceptance is not limited by discrete values as it is the case of the lumped SMD capacitors, which increases flexibility of the filter design. The obvious drawback of course is the increase in the filter volume in comparison to the lumped capacitor implementation. Another concern is the radiation loss due to open end of the coaxial line. As the wavelength approaches the diameter of the coaxial line, the radiation loss will become more pronounced. There are two approaches to overcome this problem. The first is to use a short-circuit coaxial line increasing its length to over a quarter of a guided wavelength. The second approach is to terminate the coaxial line by a capacitive gap as it is described in [11]. In this case the capacitance of the gap should be taken into account in addition to the fringing capacitance of an open-circuit coaxial line.

2.2. Excitation

The centre conductor of the feeding coaxial connector is directly connected to one of the wide walls of the waveguide and the outer conductor is connected to the opposite wall, as it is shown in Fig. 1. In some cases this excitation structure is more preferable than the traditionally used coaxial-to-planar transmission line transition followed by a planar line-to-SIW transition. Employing two series connected transitions instead of a single one is not always optimal if a coaxial interface to a SIW filter is required. Moreover, planar transmission line-to-SIW transition usually requires careful full-wave analysis and optimization, which is a time consuming task. Due to electrically small dimensions of the transition (refer to Fig. 1), the influence of the discontinuities associated with it on the overall response of the filter can be neglected in the network analysis. This will be used during the filter modelling in the following Section.

3. MODEL OF THE EVANESCENT MODE SIW FILTER

Currents and voltages are employed as measures of the fields within the evanescent mode SIW structure in the following filter analysis. Information about the behaviour of the structure is then derived using

network analysis avoiding the necessity of solving field equations.

As an example, the filter in Fig. 1 is considered here, however, the analysis of more complex structures containing several waveguide sections can also be done using this approach.

The structure of the filter is symmetric with regard to its centre. The core of the filter is a section of an evanescent mode SIW (denoted as *SIW* 1 in Fig. 1) with capacitive susceptances connected at both ends of it. The capacitive susceptances are realized in a form of open-circuited coaxial stubs *COAX*. An equivalent network representing the filter in Fig. 1 is illustrated in Fig. 3.

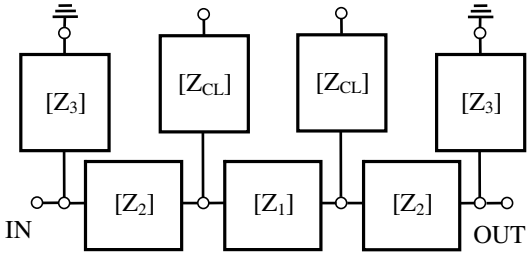

Figure 3. Filter model based on impedance matrix representation.

It consists of seven two-port networks. Each two-port network is described by an impedance matrix. *SIW* 1 is described by an impedance matrix $[Z_1]$. Coaxial line stubs *COAX* are described by impedance matrices $[Z_{\mathrm{CL}}]$. Two short sections of evanescent mode waveguide *SIW* 2 are introduced between the coaxial stubs *COAX* and feeding point for convenience of fabrication. Technologically, it is difficult to connect the coaxial stub and feeding line at the same point, and moving them slightly apart simplifies the fabrication process. Those short sections (*SIW* 2) are represented by $[Z_2]$ networks in Fig. 3.

The filter is extended with the evanescent mode waveguide sections *SIW* 3 on both sides ($[Z_3]$ networks in Fig. 3). Since these waveguide sections operate below cut-off frequency, the amplitude of the field rapidly decays over the waveguide length. The length of sections *SIW* 3 is therefore usually chosen minimizing their effect on the filter response. The outermost side of the *SIW* 3 can be left open-circuited or short-circuited. It was chosen to short-circuit the waveguide in this design to avoid any possible radiation loss. In case of open-circuit, the length of *SIW* 3 should be chosen such that the radiation from the aperture of the waveguide is negligible.

The impedance matrices for the section of evanescent mode waveguide, $[Z_i]$, and coaxial line, $[Z_{\mathrm{CL}}]$, are given by

$$[Z_i] = \begin{bmatrix} Z_{0(\mathrm{W})} \coth(\gamma_{\mathrm{W}} l_i) & Z_{0(\mathrm{W})} \mathrm{csch}(\gamma_{\mathrm{W}} l_i) \\ Z_{0(\mathrm{W})} \mathrm{csch}(\gamma_{\mathrm{W}} l_i) & Z_{0(\mathrm{W})} \coth(\gamma_{\mathrm{W}} l_i) \end{bmatrix}, \tag{1}$$

$$[Z_{\mathrm{CL}}] = \begin{bmatrix} Z_{0(\mathrm{CL})} \coth(\gamma_{\mathrm{CL}} l_{\mathrm{CL}}) & Z_{0(\mathrm{CL})} \mathrm{csch}(\gamma_{\mathrm{CL}} l_{\mathrm{CL}}) \\ Z_{0(\mathrm{CL})} \mathrm{csch}(\gamma_{\mathrm{CL}} l_{\mathrm{CL}}) & Z_{0(\mathrm{CL})} \coth(\gamma_{\mathrm{CL}} l_{\mathrm{CL}}) \end{bmatrix}. \tag{2}$$

Here $Z_{0(\mathrm{w})}$ is the characteristic impedance, γ_{w} is the propagation constant, and l_i is the length of the corresponding evanescent mode waveguide section i, with $i = 1, 2, 3$ (refer to Fig. 3). Similarly, $Z_{0(\mathrm{CL})}$ is the characteristic impedance, γ_{CL} is the propagation constant, and l_{CL} is the length of the coaxial line sections.

In order to apply transmission line theory to waveguides, a propagation constant and characteristic impedance of a particular guide configuration should be defined, as it is required by Equation (1). The considerations in Section 2 indicated that the coaxial lines are the main source of loss in the filter due to a high electric field density in them. Therefore, the attenuation due to conductor and dielectric losses in the waveguide can be neglected. The propagation constant can be expressed using the relationship for the TE_{10} mode [12] assuming that there are no magnetic materials in the waveguide

$$\gamma_{\mathrm{w}} = \sqrt{k_c^2 - k^2} = \sqrt{\left(\frac{\pi}{a}\right)^2 - 4\pi^2 f^2 \varepsilon_r \varepsilon_0 \mu_0} \tag{3}$$

Here a is the width of the waveguide, f is frequency variable, ε_r is the dielectric constant of the material filling the waveguide, $\varepsilon_0 = 8.854 \cdot 10^{-12}\,\mathrm{F/m}$, $\mu_0 = 4\pi \cdot 10^{-7}\,\mathrm{H/m}$.

Characteristic impedance in rectangular waveguide is expressed using power-voltage definition [13]:

$$Z_{0(\mathrm{W})} = 2 \cdot 120\pi \frac{b}{a} \frac{\lambda_g}{\lambda\sqrt{\varepsilon_r}} = \frac{2 \cdot 120\pi b}{a\sqrt{\varepsilon_r}\sqrt{1 - \dfrac{1}{a^2 4 f^2 \varepsilon_r \varepsilon_0 \mu_0}}}, \tag{4}$$

where b is the narrow side of the waveguide which corresponds to the height of the substrate in the case of SIW realization.

It should be noted that $[Z_i]$ in Equation (1) completely describes the behaviour of the TE_{10} mode in the dielectric-filled lossless waveguide below as well as above the cut-off. This allows to use this expression for analysis of waveguide filters in a wide frequency range (at least at frequencies below the cut-off of the second propagating mode).

The characteristic impedance of a coaxial cable filled with dielectric in Equation (2) [12]:

$$Z_{0(\mathrm{CL})} = \frac{1}{2\pi}\sqrt{\frac{\mu_0}{\varepsilon_r\varepsilon_0}} \ln\left(\frac{d_o}{d_i}\right), \tag{5}$$

Here ε_r is the dielectric constant of material filling the coaxial cable; d_o and d_i are the diameters of the outer and inner conductors.

The propagation constant

$$\gamma_{\mathrm{CL}} = \alpha_c + \alpha_d + j\beta = \frac{1}{2Z_{0(\mathrm{CL})}}\left(\frac{1}{d_o} + \frac{1}{d_i}\right)\sqrt{\frac{f\mu_0}{\pi\sigma}} + \pi f\sqrt{\varepsilon_r\varepsilon_0\mu_0}\mathrm{tg}\delta + j2\pi f\sqrt{\varepsilon_r\varepsilon_0\mu_0}, \tag{6}$$

where σ is the conductivity of metal and $\mathrm{tg}\delta$ is the loss tangent of dielectric material [12].

Substituting Equations (3)–(5) into Equations (1)–(2) allows to calculate the response of the filter applying a network analysis to the network in Fig. 3. Since this calculation is efficient in terms of computational time, the design of the filters can be done using an iterative approach [14].

4. DESIGN EXAMPLE

An example of a microwave filter, as the one shown in Fig. 1, has been designed. The filter suppose to have maximally flat response with a bandwidth of 2.5% and operating frequency around 1.4 GHz. The implemented substrate is RO 4003 [15] with 1.52 mm thickness. Relative permittivity of the substrate material is 3.55. The implemented coaxial cable for stubs *COAX* is EZ 141 [16], having a copper conductor ($\sigma \approx 5.8 \cdot 10^7$ S/m). The centre conductor diameter is 0.92 mm, and the outer conductor diameter is 3 mm. The cable is filled with PTFE dielectric ($\varepsilon_r \approx 2.1$, $\mathrm{tg}\delta \approx 0.002$). These design requirements and implemented materials result in the following parameters of the model:

$$\begin{aligned} &f_0 = 1.4\,\mathrm{GHz}; \delta f = 2.5\%; a = 25\,\mathrm{mm}; b = 1.52\,\mathrm{mm};\\ &d_i = 0.92\,\mathrm{mm}; d_o = 3\,\mathrm{mm}; \sigma = 5.8 \cdot 10^7\,\mathrm{S/m}; \mathrm{tg}\delta = 0.002;\\ &\varepsilon_r = 3.55 \text{ (for waveguide, Equations (3) and (4))};\\ &\varepsilon_{\mathrm{r}} = 2.1 \text{ (for coax. line, Equations (5) and (6))}. \end{aligned} \tag{7}$$

The width of the SIW, $a = 25$ mm, results in a cut-off frequency of approximately 3.2 GHz.

Synthesis of evanescent filters, namely, analytical determination of filter parameters from low-pass prototype is not trivial and requires iterative procedure [17]. Therefore the iterative design approach is directly applied here to the network in Fig. 3 to find the parameters of the filter, as described below.

The parameters (7) are substituted in Equations (3)–(6), which provide basis for transmission line impedance matrices (1)–(2). These matrices describe corresponding components of the network in Fig. 3. This network is then used to synthesize the filter by optimization [14]. During optimization, the lengths of the SIW sections *SIW* 1, *SIW* 2, *SIW* 3 (described by $[Z_1]$, $[Z_2]$, and $[Z_3]$) and coaxial line *COAX* (described by matrix $[Z_{\mathrm{CL}}]$) are iteratively selected. The optimization concerns the following parameters of the model (refer to Equations (1)–(2)):

$$l_1, l_2, l_3, l_{\mathrm{CL}}. \tag{8}$$

The obtained lengths of the waveguides and coaxial lines are listed in Table 1.

Table 1. Lengths of the filter components[a].

Parameter	l_1	l_2	l_3	l_{CL}
Value, mm	18.3	3	20	32.8

[a]The total length of the filter is $l_1 + 2l_2 + 2l_3 = 64.3$ mm.

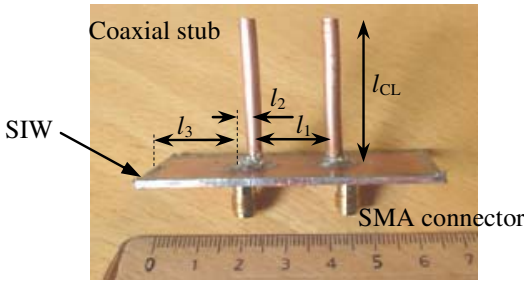

Figure 4. Photograph of the evanescent mode SIW filter with coaxial stubs.

The designed filter is then fabricated and tested. A photograph of the realized filter is shown in Fig. 4.

If smaller volume is required, coaxial stubs can be bent. In that case, eventual change in the input impedance of the stub should be taken into account.

The measured magnitudes of the scattering parameters are shown in Fig. 5. The measured minimum insertion loss of the filter is under 2.1 dB. The considerations above indicated that the loss mainly stems from the coaxial stubs due to finite conductivity of the copper. These losses can be decreased by choosing coaxial cable with larger diameter, or increasing the width of the waveguide which will result in lower current density in the coaxial lines. This will of course lead to an increase in the filter dimensions.

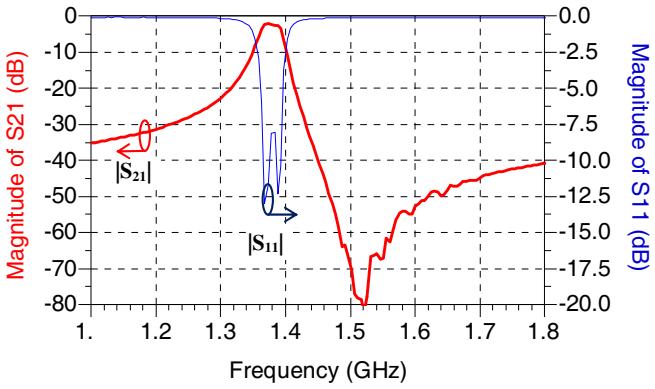

Figure 5. Measured response of the filter in Fig. 4. The 3 dB bandwidth is approximately 35.5 MHz, which corresponds to 2.6% of fractional bandwidth at a centre frequency of approximately 1.38 GHz.

Even though the fabricated structure exhibits a filtering behaviour, one can note that there is a room for reflection loss improvement.

The measured and predicted scattering parameters of the filter in a wide frequency range are shown in Fig. 6.

As one can note, the filter exhibits a transmission zero on the upper side of the pass-band, which results in a sharp roll-off. The frequency of the transmission zero corresponds to the frequency where the electrical length of the coaxial stub is approximately a quarter of a guided wavelength. The frequency of this transmission zero is relatively difficult to control since the length of the stub also defines the

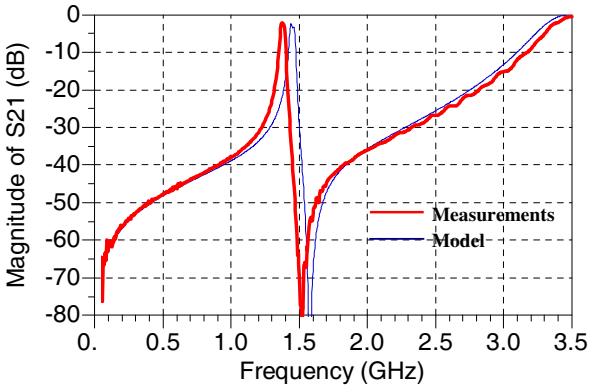

Figure 6. Broadband response of the filter.

capacitance required for the evanescent mode propagation. It would be also preferable to generate a transmission zero at the lower pass-band side in order to generate a quasi-elliptic behaviour. There is, however, no simple way to realize that in the present structure.

The filter model has a reasonable accuracy in a wide frequency range. There is, however, still a visible discrepancy between the calculated and measured response of the filter in Fig. 6. The calculated minimum insertion loss is 2.4 dB, which is 0.3 dB more pessimistic than the measurements. The calculated response is shifted up in frequency by approximately 66.7 MHz, which corresponds to 4.86% error. It was observed that the filter is sensitive to the length of the coaxial stubs, which can be used for fine tuning of the centre frequency. The discrepancy between the calculated and measured response partially results from the fact that effects of the open end of the coaxial stubs as well as the short-circuited waveguide terminations were not included in the model for simplicity reasons. A higher accuracy can be achieved, if necessary, by using a full-wave electromagnetic analysis. This is of course will be more computationally expensive.

It can be noted that the upper stop-band degrades above the transmission zero, exhibiting a low rejection approximately at the cut-off frequency of the implemented waveguide. The frequency of this spurious response is defined by the cut-off frequency of the dominant mode in the implemented waveguide, *SIW* 1 (3.2 GHz in this case) and depends on its width a. Above this frequency the wave easily propagates as TE_{10} mode. This suggests several approaches to improving the upper stop-band response. The straightforward way to control the cut-off frequency of the waveguide is to change its width, a. The alternative way is to introduce a discontinuity into the waveguide. In this way the filter can also be further miniaturized as also indicated in [9]. The approach of using inductive posts for these purposes is discussed in the following Section.

5. STOP-BAND IMPROVEMENT USING INDUCTIVE POSTS

Introducing an inductive post into an evanescent mode waveguide, as it is shown in Fig. 7, increases the equivalent inductance of the waveguide and potentially allows reducing the length of the waveguide section required in the filter.

Increase in the inductance decreases coupling between the resonators formed by coaxial stubs and evanescent mode SIW sections. The length of the waveguide section should be decreased in order to compensate for that. The inductive post increases the cut-off frequency of the propagating mode which should improve the upper frequency stop-band characteristics.

In order to test these speculations, the model developed in Section 3 has been extended including a network describing the inductive post. The resulting model for the structure in Fig. 7 is shown in Fig. 8. Here, the evanescent mode SIW section is split into two equivalent parts, which are described by $[Z_1]$. The inductive post is described by matrix $[Z_p]$. Since it is a one port component, the impedance matrix contains only one impedance coefficient

$$[Z_p] = [1/j \cdot B], \tag{9}$$

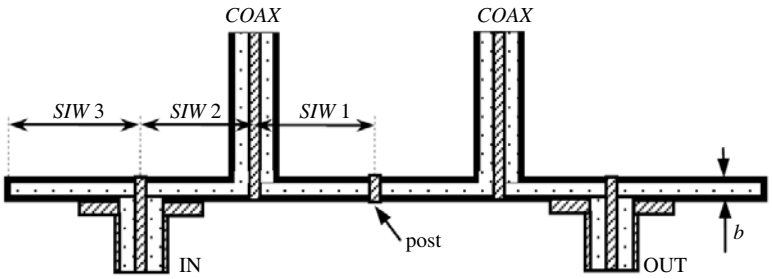

Figure 7. Sketch of the filter cross-section (not to scale).

where B is the susceptance of a single post centred in the guide [8] given by

$$B = -\frac{2\lambda_g}{aZ_{0(w)}\left[\ln\left(\frac{a}{11.6067r} + \frac{0.2076a^2}{\lambda^2}\right)\right]}. \tag{10}$$

Here

$$\lambda_g = \frac{2\pi}{\beta} = \frac{2\pi}{\sqrt{k^2 - \left(\frac{\pi}{a}\right)}} = \frac{2\pi}{\sqrt{4\pi^2 f^2 \varepsilon_r \varepsilon_0 \mu_0 - \left(\frac{\pi}{a}\right)^2}}, \quad \lambda = \frac{2\pi}{k} = \frac{1}{f\sqrt{\varepsilon_r \varepsilon_0 \mu_0}}, \tag{11}$$

r is the radius of the post and $Z_{0(\mathrm{w})}$ is found from Equation (4). The post in SIW is realized in a form of a metalized via hole.

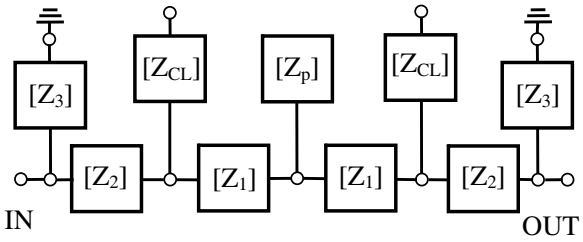

Figure 8. Filter model based on impedance matrix representation.

The length of *SIW* 1 and *COAX* is adjusted using the model in Fig. 8 such that the centre frequency of the filter corresponds to the frequency of the original filter. The corresponding parameters of the filter are listed in Table 2.

Table 2. Parameters of the components[a] for the filter in Fig. 7.

Parameter	$\mathbf{l_1}$	$\mathbf{l_2}$	$\mathbf{l_3}$	$\mathbf{l_{CL}}$	**r**
Value, mm	12.5 / 2	3	20	33.1	0.4

[a]The total length of the filter is $2l_1 + 2l_2 + 2l_3 = 58.5$ mm.

The length of the filter is reduced by 5.8 mm shortening the evanescent SIW section between stubs by 31%. The calculated responses of the filters with and without the post are given in Fig. 9. It is seen, that the rejection performance of the filter is slightly improved by adding a post. However, the price to pay is an increase in the insertion loss.

In order to validate presented calculations, a filter in Fig. 7 has been fabricated and tested. The measured performances for both filters (with and without the post) are shown in Fig. 10. As predicted, the upper stop band response improves. In some applications, however, even a better stop-band performance still might be required. Further stop-band improvement can be achieved by open-circuiting the waveguides *SIW* 3 exploiting natural radiation from the open ended waveguide at frequencies above the cut-off. This approach, however, has been left out of the scope of this paper.

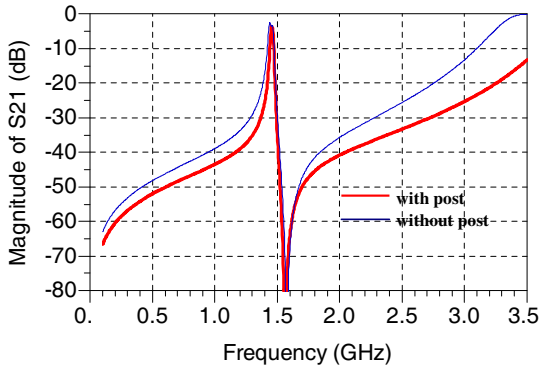

Figure 9. Response of the filter with and without a post. Calculated using models developed in Sections 3 and 4.

The filter exhibits a transmission zero as for the case of the original filter.

The measured minimum insertion loss, however, degraded by 0.8 dB and corresponds to 2.9 dB for the filter with the post.

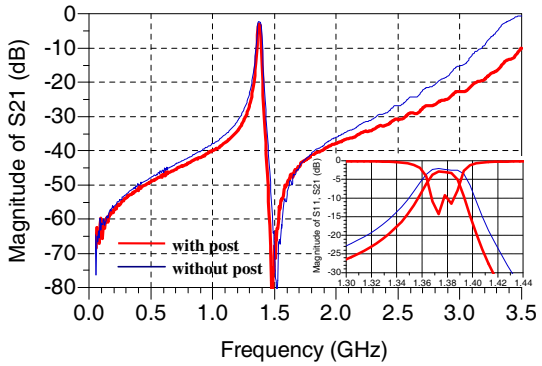

Figure 10. Measured response of the band-pass filters in Fig. 1 and Fig. 7. The bandwidth has reduced to 25 MHz, which corresponds to a fractional bandwidth of approximately 1.8%.

Another impact of the post is the reduction of the coupling between two resonators formed by coaxial stubs *COAX* and waveguide sections *SIW 1*. The measured magnitude of S_{11} at the centre frequency is below -9 dB, which could still be improved. This can be achieved by either adjusting the distance between the feed point and a coaxial stub, or choosing an alternative excitation method.

In conclusion, the implementation of the post allows for up to 10 dB better stop-band rejection and more compact design, however, leads to a degradation of in-band performance in comparison to the structure without the post.

6. CONCLUSION

It is shown that the evanescent mode waveguide can be integrated into a single layer substrate using capacitive susceptances in the form of externally connected coaxial stubs. A microwave filter based on these principles was developed and tested in order to investigate this experimentally. The presence of the coaxial stubs results in a transmission zero improving overall selectivity of the filter. The filter has a spurious response above the cut-off frequency of the implemented SIW. It is possible to improve the upper stop-band of the filter up to 10 dB by introducing an inductive post at the expense of insertion loss, which degraded by 0.8 dB. The modified filter is shorter in comparison to the original filter due to reducing the length the evanescent mode SIW section between the stubs by 31%.

A model for the filters is developed. It is efficient in terms of computational time, which allows filter synthesis by optimization.

It was observed that the filters are sensitive to the length of coaxial stubs. Using this property, a fine tuning of the filter can be achieved. This feature could also be used for constructing tuneable filters.

REFERENCES

1. Shen, T. and K. A. Zaki, "Length reduction of evanescent-mode ridge waveguide bandpass filters," *Progress in Electromagnetics Research*, Vol. 40, 71–90, 2003.
2. Kirilenko, A., L. Rud, V. Tkachenko, and D. Kulik, "Evanescent-mode ridged waveguide bandpass filters with improved performance," *IEEE Transactions on Microwave Theory and Techniques*, Vol. 50, No. 5, 1324–1327, May 2002.
3. Wu, L.-S., X.-L. Zhou, and W.-Y. Yin, "Evanescent-mode bandpass filters using folded and ridge substrate integrated waveguides (SIWs)," *IEEE Microwave and Wireless Components Letters*, Vol. 19, No. 3, 161–163, March 2009.
4. Wu, L.-S., X.-L. Zhou, W.-Y. Yin, L. Zhou, and J.-F. Mao, "A substrate-integrated evanescent-mode waveguide filter with nonresonating node in low-temperature Co-fired ceramic," *IEEE Transactions on MTT*, Vol. 58, No. 10, 2654–2662, October 2010.
5. Huang, L., I. D. Robertson, W. Wu, and N. Yuan, "Substrate integrated waveguide filters with broadside-coupled complementary split ring resonators," *IET Microw. Antennas Propag.*, Vol. 7, No. 10, 795–801, 2013.
6. Dong Y., C.-T. M. Wu, and T. Itoh, "Miniaturised multi-band substrate integrated waveguide filters using complementary split-ring resonators," *IET Microw. Antennas Propag.*, Vol. 6, No. 6, 611–620, 2012.
7. Zhang, Q.-L., W.-Y. Yin, and S. He, "Evanescent-mode substrate integrated waveguide (SIW) filters implemented with complementary split ring resonators," *Progress In Electromagnetics Research*, Vol. 111, 419–432, 2011.
8. Craven, G. F. and C. K. Mok, "The design of evanescent mode waveguide bandpass filters for a prescribed insertion loss characteristic," *IEEE Transactions on MTT*, Vol. 19, No. 3, 295–308, March 1971.
9. Craven, G. and R. Skedd, *Evanescent Mode Microwave Components*, 180, Artech House, 1987.
10. Snyder, R. V., "Inverted-resonator evanescent mode filters," *IEEE MTT-S Microwave Symposium Digest*, Vol. 2, 465–468, 1996.
11. Marcuvitz, N., *Waveguide Handbook, IEEE Electromagnetic Waves Series*, 446, 1986.
12. Ramo, S. and J. R. Whinnery, *Fields and Waves in Modern Radio*, 2nd Edition, John Wiley and Sons, New York, 1962.
13. Rizzi, P. A., *Microwave Engineering: Passive Circuits*, Prentice-Hall, Englewood Cliffs, NJ, 1988.
14. Hong, J.-S., and M. J. Lancaster, *Microstrip Filters for RF/Microwave Applications*, 457, John Wiley & Sons, Inc., 2001.
15. *RO4000 Series High Frequency Circuit Materials*, 8, Datasheet, Rogers Corp..
16. Coaxial Cable: EZ_141, Data Sheet, 2, Huber+Suhner.
17. Jarry, P., J. Beneat, E. Kerherve, and H. Baher, "New class of rectangular and circular evanescent-mode waveguide filter," *International Journal of RF and Microwave Computer-Aided Engineering*, Vol. 8, No. 2, 161–192, March 1998.